Stability Considerations for a Synchronous Interconnection of the North American Eastern and Western Electric Grids

Thomas J. Overbye
Texas A&M University
overbye@tamu.edu

Komal S. Shetye
Texas A&M University
shetye@tamu.edu

Jess Wert
Texas A&M University
wert@tamu.edu

Hanyue Li
Texas A&M University
hanyueli@tamu.edu

Casey Cathey
Southwest Power Pool Inc.
ccathey@spp.org

Harvey Scribner
Southwest Power Pool Inc.
hscribner@spp.org

Abstract

This paper presents some of the stability considerations for an ac interconnection of the North American Eastern and Western electric grids. Except for a brief time around 1970, the North American Eastern and Western grids have operated asynchronously, with only small power transfers possible through a few back-to-back HVDC ties. This paper provides results from a study showing that an ac interconnection may be possible with only modest changes to the existing transmission grid. The paper's main focus is on the dynamic aspects of such an interconnection. The paper also shows how newer visualization techniques can be leveraged to show the results of larger-scale, long duration dynamic simulations. Results are given for a 110,000-bus model of the actual North American electric grid and an 82,000-bus synthetic grid.

1. Introduction

This paper presents some of the stability considerations for an ac interconnection of the North American Eastern and Western electric grids. Currently most of the electricity used in North America (NA) is supplied by four major interconnects, with each operating at 60 Hz but asynchronous with each other. The four grids are the Eastern Interconnect (EI), the Western Electricity Coordinating Council (WECC), the Electric Reliability Council of Texas (ERCOT), and the Quebec Interconnection. All of these ac networks are internally synchronized and are linked to at least some of the others only through dc ties.

For several years, starting on February 7, 1967, the EI and WECC (then known as Western System Coordinating Council with its name changed in 2002) were operated as a single electric grid, with the interconnection motivated by a desire to improve electric grid reliability as a result of the November 1965 Northeast Blackout. While this interconnection worked initially, within months problems became apparent including oscillations on the western side and large inadvertent exchanges [1] [2]. This led to the overloading of transmission facilities, system breakups, reduced transmission capacity and a final removal of the ac interconnection in the early 1970's. Since then several back-to-back, high voltage dc (HVDC) facilities have been constructed along the seam between the EI and WECC, allowing for up to 1.5 GW of east-west power transfer while the two grids operate asynchronously.

Over the years there have been several studies looking at a stronger connection between the EI and WECC, with some of this work focused on the economic or resource planning aspects [3], [4], and some on the use of HVDC for transmission expansion and design [5], [6]. In particular [6] focused on leveraging dc systems through upgrading the existing back-to-back (B2B) dc ties and building some new long distance HVDC lines. While this included rigorous analyses considering future capacity and carbon policies, a key area of improvement that this study did not consider is stability analysis.

The feasibility of a new synchronous interconnection has been studied less frequently [7]. This is partially because as a result of the interconnection failure in the early 1970's an ac connection has been viewed as, "like tying two elephants together with rubber bands; they can only go so far in opposite directions before the rubber bands snap" [8]. However, there has been significant growth since the 1970's in transmission and generation plants along the EI-WECC boundary. There have also been many changes in technology, particularly with the now widespread application of power system stabilizers, and greatly improved electric grid monitoring and control. The need for more up-to-date assessments with improved stability models is identified in [7] and [9]. Given the importance of system stability to any consideration of again operating these grids synchronously, this paper builds on and extends the earlier results presented from a 2020 study on an ac interconnection of the EI and WECC in [10] and [11]. PowerWorld Simulator Version 22 is used for all the simulation results shown here, in part due to its ability to model the stability models used in both the EI and WECC grids, and also its ability to efficiently visualize engineering results.

URI: https://hdl.handle.net/10125/79776
978-0-9981331-5-7

The paper is organized as follows. After this introduction the second section presents the electric grid models used in the study. Given that some information about the actual electric grids models used is designated as Critical Energy/Electricity Infrastructure Information (CEII) [12] and hence not fully publicly available, the paper also presents some results based on non-CEII synthetic grids. The third section provides some overview results from the study based on the actual grid models, whereas the fourth section provides more detailed results on the study's methodology and associated visualizations using the synthetic grids. Then the fifth section summaries the paper and discusses some future directions.

2. Electric Grid Models

Given that the overall goal is to consider the stability aspects of an ac interconnection of the EI and WECC, full detail power flow and stability models for both interconnects have been utilized. However, since much of the information about these actual grids is considered CEII and hence its publication restricted, the paper also considers the stability aspects of an interconnection of two large-scale synthetic grids [13], [14], [15].

For the real grids two different base case conditions are considered, one representing a heavy loading scenario and one representing a light loading scenario. Each of these base cases was created by combining an 87,000 bus (87K) EI grid model with a 23,000 bus (23K) WECC model in which each contained power flow and transient stability level dynamic models; the buses, areas, zones and owners in the WECC have been renumbered to avoid overlap. Also, some WECC remedial action schemes (RASs) have been included [16]. Each case has about 110,000 buses, 160 operating areas (areas), and 40,000 geo-mapped substations. The heavy load case has about 848 GW of total generation and 828 GW of load, while the light load case has 419 GW of generation and 408 GW of load. In both cases a little more than 20% of the total load and generation is in the WECC.

The grids were then combined using nine short ac connections at locations in which the EI and WECC are already close geographically (often within the same substation). These interconnections ranged from Montana in the north to New Mexico in the south (while the Canadian electric grid is represented in the models, no new connections were added in Canada). Overall this new interface had one 345 kV connection, four 230 kV connections, three 345/230 kV transformers and one 230/161 kV transformer. Figure 1 shows a high-level transmission view of the combined grids with the different colors used to indicate the different nominal voltage levels (green for above 700 kV, orange for 500 kV, red for 345 kV, blue for 230 kV and black for lower voltages). In the figure the substations closest to the interface are highlighted.

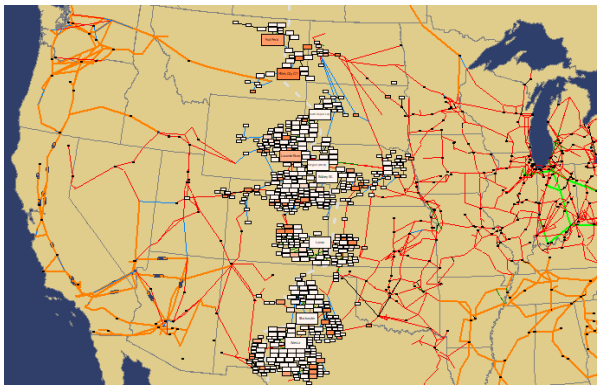

Figure 1: Overview of 110K Grid Model

To provide a feel for the overall 110K grid, Figure 2 provides a geographic data view (GDV) [17], [18] visualization of the grid's areas for the initial heavy loading scenario in which the size of each area GDV is proportional to the area's generation and the GDV's color is based on its amount of MW exports (with red for net exports and blue for imports). The Delaunay triangulation based wide-area flow visualization method of [19] is then used to show how the power is flowing between the areas, with the size of the green arrow proportion to the real power flow. In the figure it is apparent both that the EI and WECC are joined and that there is relatively little flow across this interface (in the starting heavy load scenario the net interface flow has been set to zero).

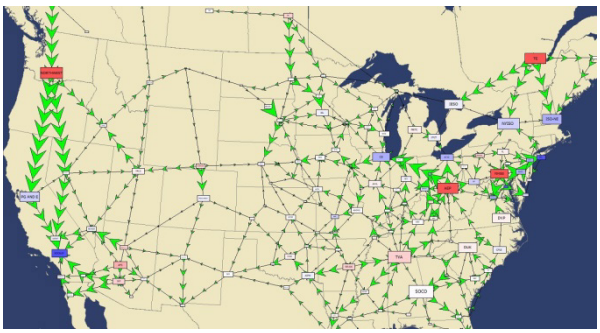

Figure 2: Inter-Area Power Flows for 110K Model

To provide more methodology and visualization details without compromising CEII, in this paper results are also demonstrated using an 82,000 (82K) synthetic grid that had been constructed to cover the contiguous US (CONUS). This grid, whose oneline is shown in Figure 3, was constructed to duplicate the overall CONUS electric generation and load

distribution, and to also have three separate ac interconnections whose footprints match the CONUS portions of the EI, WECC and ERCOT. However, the transmission system is entirely fictitious; the same Figure 1 color scheme is used in Figure 3 to indicate the nominal transmission voltage levels. The dividing line between the east and west grids is indicated by the thick black line in Figure 3. For this project the east and west footprint portions were joined together using eight transmission lines and transformers given in Table 1. Figure 4 shows the same information as Figure 2 except for the 82K grid. The grid model is available at [20], and for completeness the ERCOT footprint portion is included in the model but since it operates asynchronous from the other two it did not impact the results.

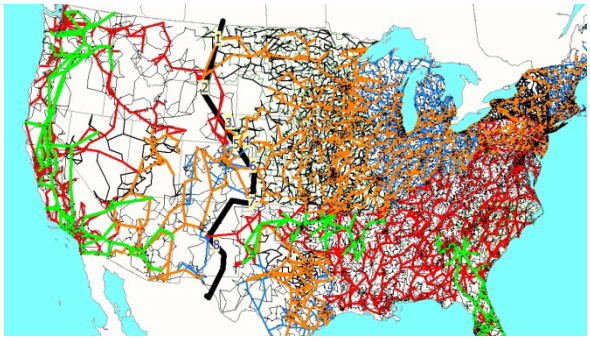

Figure 3: 82,000 (82K) Synthetic Electric Grid Oneline

Table 1: 82K East-West Interconnection Points

No.	West Bus (kV)	East Bus (kV)	US State	Limit (MVA)
1	Glasgow (138)	Fort Peck (500)	MT	250
2	Hardin (345)	Colstrip (500)	WY	750
3	Wheatland (345)	Scottsbluff (500)	WY	600
4	Peetz (500)	Sidney (500)	NE	800
5	New Raymer (500)	Kimball (500)	CO	800
6	Burlington (500)	Goodland (500)	CO	800
7	Lamar (500)	Johnson (161)	CO	350
8	Willard (230)	House (345)	NM	450

Before getting into the results, it is important to stress two germane characteristics of both the actual and the synthetic grids. First, as noted earlier with the elephant and rubber band reference, a proposed ac interconnection of the EI and WECC involves connecting two quite large grids using connections that can only carry a small percentage of the total load. Second, while both the EI and WECC are large grids, they are most definitely not equal in size, with the EI having about four times the load of the WECC. As noted in the next sections this results in an asymmetry in their responses to the contingencies.

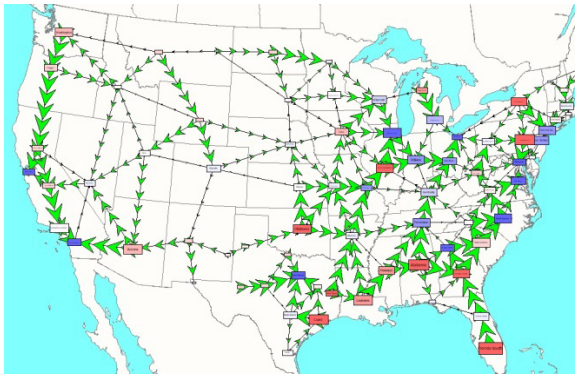

Figure 4: 82K Grid Inter-Area Power Flows

3. Actual Grid Stability Results

The focus of the project and hence this paper is on grid stability assessed using time-domain simulations. Electric grid time-domain simulations can be divided based upon the time scale of the underlying dynamics with [21] presenting four groups, starting with wave phenomena (with a time scale of less than a microsecond) and going out to thermodynamic (ranging up to many hours). The time-domain simulations considered here are in the middle of this range, a scale for which the electric grid is modeled using a phasor representation. As noted in [22] and [21], this considers aspects of rotor angle stability, voltage stability, frequency stability, and to some extend converter driven stability. Sub-synchronous resonance [23] was not considered. The integration step size used is ½ electrical cycle (8.333 ms), though the use of multirate methods [24], [25], [26], [27] allows for accurate modeling of the much faster models associated with devices such as exciters, loads and some renewable generators. The simulations considered here have a fixed duration ranging from seconds to several minutes.

One of the challenges of this project is dealing with the sheer magnitude of the size and complexity of the grids, and the amount of data that is produced during the time-domain simulations. For the actual system the model contains about 110,000 buses, 13,700 generators, 246 different types of dynamics models, more than 61,000 dynamic model instances, and more than 200,000 differential equations. A reason for the larger number of dynamic model types is due to the original dynamics data coming from two separate electric grid models (i.e., EI and WECC) with

potentially different types of models used in each. For example there are slight differences in the common EXST1 exciter model between what is used in the EI and the WECC models. However, the software used here supports both types. The situation is somewhat simplified for the synthetic grid, which has 80,000 buses, 25 different types of dynamics models, 60,000 dynamic model instances and 237,000 differential equations. Determining how best to present this information has been a crucial part of this work and is presented more fully in the next section.

To consider the stability implications of an EI-WECC ac interconnection, a wide variety of different time-domain simulations have been run on both the heavy and light load scenarios under a variety of different interface loading scenarios for a wide variety of different types of contingencies. Example contingencies included faults, transmission element outages and generator outages including up to 10 GW of generation loss in the EI. Whiles some of these contingencies involved just a single element (such as a single generator outage), most involved multiple elements, with the most severe involving a simultaneous outage of eight large generators.

The key limiting characteristic on interconnecting the EI and WECC is during generator loss contingencies in the WECC approximately 80% of the lost power will flow through the ac interface from east to west since the governor response takes place uniformly through the interconnect and most of the generation capacity and hence the associated governor response is east of the interface. During generator contingencies in the EI approximately 20% of the lost power flows through the interface from west to east, but since this percentage is substantially smaller, this is viewed as a much less severe constraint. Hence the most severe contingencies tended to be in the WECC.

As an example of a severe contingency, Figure 5 shows the time variation in the interface MW flow for the loss of 2700 MW of generation in the WECC, with positive flow in the figure from east to west. As can be seen the power across through the interface increases from a pre-contingent value of 150 MW to around 2600 MW, and then seems to settle at around 2200 MW. That is, a total of nearly 2100 MW of additional power flows on the ac ties from the EI to the WECC to make up for the 2700 MW outage in the WECC. Thus the change in the interface flow is about 80% of the generation lost.

This governor response flow issue is fundamental to interconnecting large grids and does require any interface joining two such larger grids be able to handle this increase in flow, at least until the automatic generation control (AGC) can respond. In particular for the EI and WECC connection there should to be more than just a few tielines, with nine studied here. The small number of tie-lines associated with the original interconnection in 1967 was probably a key reason for its poor performance.

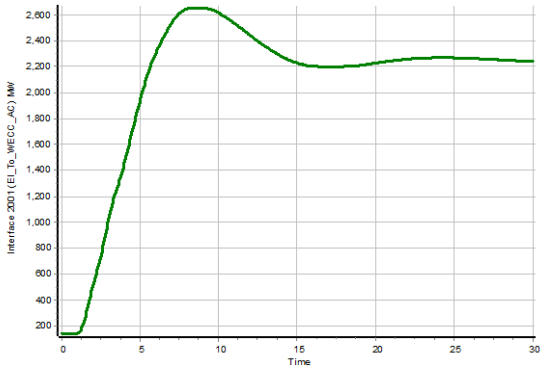

Figure 5: AC Tie Interface Flow (East to West Positive)

During a contingency a benefit of this rapid change in the interface tie flow is its positive impact on the WECC frequency response for WECC generator loss contingencies. As an example, Figure 6 compares the frequency variation at five locations both with the grids joined (corresponding to the thick lines in the figure) and with the grids separate (corresponding to the thin lines in the figure with the same color). The black line response is for a location close to the contingency, the purple and brown lines for other WECC locations, the green line for an EI location close to the interface, and the red line for an EI location in New England. Within the first second or two there is little difference, but within seconds makeup power rapidly flows in from the east. While this causes some decrease in the EI frequencies, as noted in the figure the impact is modest.

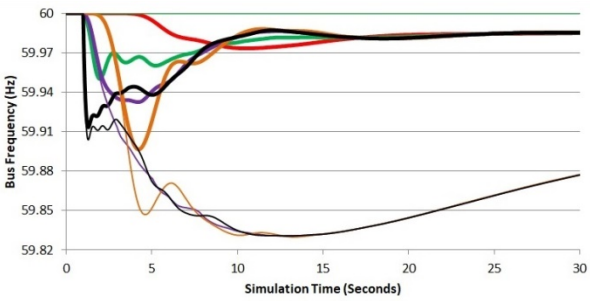

Figure 6: Frequency Response With and Without Ties

To show the overall system response to this contingency for the joined grids, Figure 7 plots the bus frequencies for the 23K buses in the WECC, and using the same scale, Figure 8 for the 87,000 buses in the EI. Clearly the impact of this event on the EI is minimal

and the interface flows help with the WECC frequency response. This is a characteristic of essentially all the contingencies: the impact in the EI is quite modest for WECC contingencies and not much changed from asynchronous operation for EI contingencies.

Switching to voltage magnitudes, Figure 9 shows the voltage magnitude variation for all the WECC buses, whereas Figure 10 shows the same data except showing the voltage magnitude deviation from its initial value. The seemly steady-steady change in many of the voltage magnitudes is due to the change in the system operating point as a result of the contingency and subsequent change in flows due to the generator responses. While none of the voltage magnitude deviations in Figure 10 is overly excessive, clearly additional scrutiny is warranted. This will be partially addressed in this section by including the generator governor response and partially with the visualizations presented in the next section.

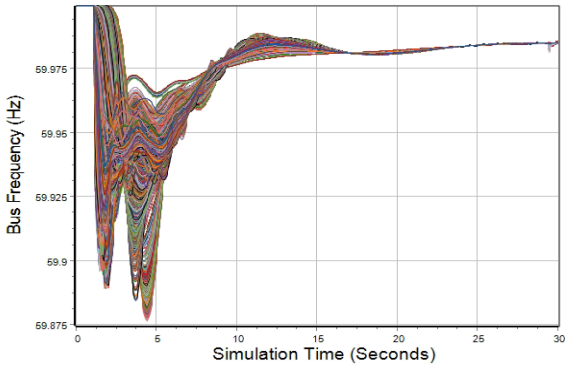

Figure 7: Envelope of WECC Frequency Response

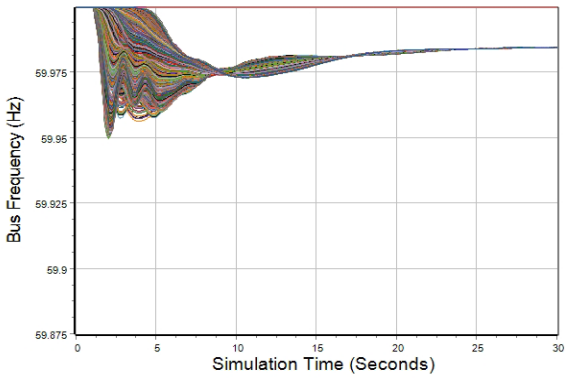

Figure 8: Envelope of EI Frequency Response

Typically time-domain stability simulations last no more than about thirty seconds, which is sufficient time to see if the system settles to a new quasi-steady state equilibrium point, and usually they do not include the AGC response that takes place on the order of minutes to restore the system frequency to 60 Hz and to rebalance the balancing authority (BA) area control error (ACE). However, for the more exploratory studies considered here, in which the grids are operated in a new fashion, some of the studies have been extended to include the ACE calculation, defined for BA_i as

$$ACE_i = P_{i,actual} - P_{i,sched} - 10\beta_i(f_{act} - f_{sched})$$

where $P_{i,actual}$ is the actual MW interchange for BA_i, $P_{i,sched}$ is its scheduled interchange, β_i is the BA's frequency bias (it has a negative sign, units of MW/0.1 Hz and is about 0.8% of the magnitude of the peak load or generation), f_{act} is the actual frequency in Hz sensed at a bus and f_{sched} is the scheduled frequency for the entire system, assumed here to be 60 Hz.

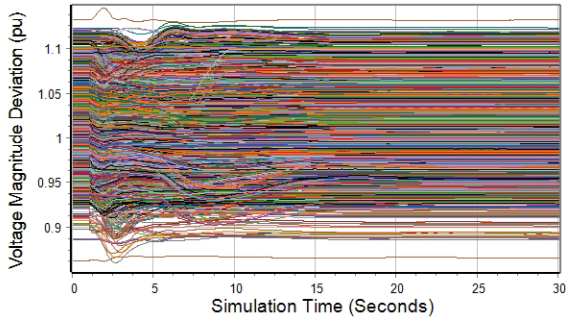

Figure 9: Actual WECC Voltage Magnitude Response

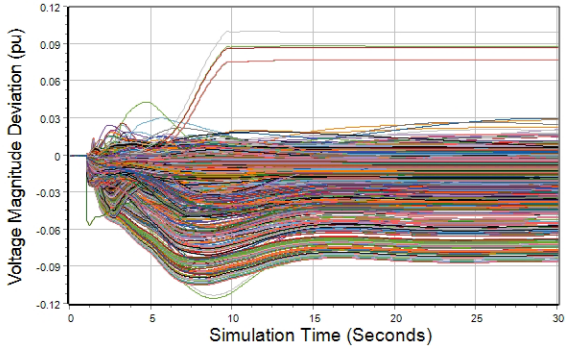

Figure 10: WECC Voltage Deviation

While actual AGC modeling can be quite complex, nevertheless since the used simulation software provides some support for more generic AGC modeling, this response is included in some of the studies to consider how the interconnected grid recovered. This was setup by considering all the power flow areas to be BAs, defining all of them as being on AGC control, assigning to each a default β value (equal to about 1% of the peak load in the area with a negative sign), a frequency measurement bus, an ACE MW deadband and a set of scheduled transactions. For each area the unspecified transactions are set so the

starting ACE for each area is zero. In addition, each generator also needs an AGC controller. The AGC controller has a MW minimum and maximum value, and a participation factor. Given that this information is not available in the models used here, defaults were used in the initial studies (min/max values from the power flow, and its participation factor proportional to is maximum MW value). Then during the simulation the area ACE is calculated, with the ACE error sent to the generator AGC controllers, with the desired MW control change proportional to its participation factor. This error is then used to change the governor setpoint.

For the simulation presented here the contingency is again a loss of generation in the WECC. Initially, as before, the change in the generation is handled by the governor response. But then in these extended simulations bilateral transactions are implemented between the area that lost the generation and other nearby areas, with the transactions ramping up over a specified time period. For the initial AGC simulations, which ran for several minutes with the transactions starting at 30 seconds and ramping over two minutes, using the standard integration step size of ½ electrical cycle, a 0.08 Hz oscillation was observed. This was concerning since low frequency 0.07 Hz oscillations had been reported with large-scale interconnection studies in Europe [28]. However, using the modal analysis techniques from [29] and [30], the source of this oscillation was determined to be from a single large unit more than a 1000 miles from the interface with what appears to be incorrectly tuned governor PID values. The oscillation was removed when this single generator was taken off of AGC control.

Figure 11 shows the change in the interface flow for the previous WECC generator loss contingency, and then with AGC implemented with the lost power made up by modeling transactions with other areas in the WECC. The result is the interface flow ramped back down to its original value and the system frequency is restored to 60 Hz. Figure 12 shows the change in several of the WECC bus voltages.

4. Visualization of Simulation Results

A key challenge associated with interpreting the results of these large-scale, time-domain simulations is understanding what is going on. This is a particular issue for this study since changes could be occurring almost anywhere in a now continent spanning grid. As a result of this challenge several new visualization approaches have been developed with some of these results previously presented in [18], [31]. This section briefly builds on and expands these results using the previously mentioned 82K synthetic grid, whose model and associated visualizations are available at [20]. While over the course of the project this grid had been used for several different studies, the results presented here are associated with the rather severe contingency in the western portion of the system, the outage of 2800 MW of generation located at buses 2040844, and 2040845 that is assumed to occur at a simulation time of 1.0 seconds.

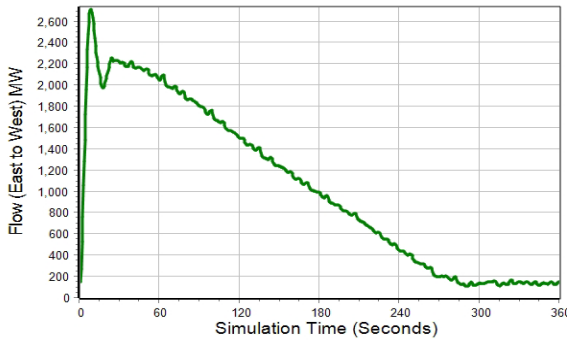

Figure 11: Interface Flow for Simulation with AGC

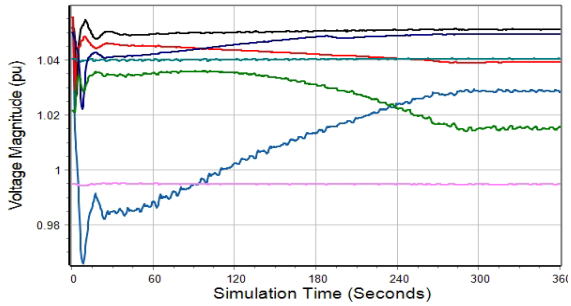

Figure 12: Simulation with AGC Bus Voltage Variation

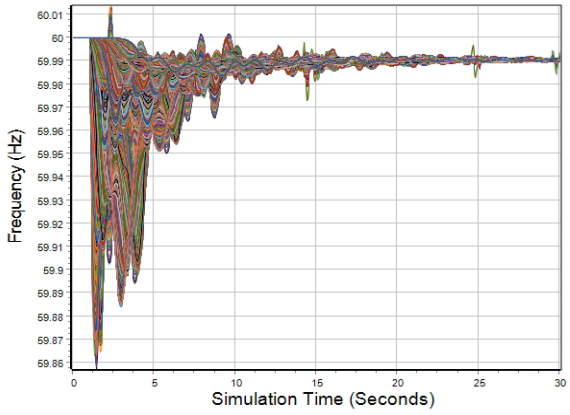

Figure 13: Envelope of 82K Frequency Response

An overall summary of the system response for this contingency is shown in Figure 13 and Figure 14, which respectively show the bus frequencies and the bus per unit voltage magnitude deviation for all 80,000 buses. An advantage of such comprehensive plots is they provide bounds on the overall system response. However, a disadvantage is because of the large

number of signals shown many signals are hidden and it is hard to get a feel for the overall distribution of the signal values. For example, a statistical analysis of the data indicates that the short spikes shown in Figure 13 at 25 and 30 seconds are due to spurious behavior at just two buses with very small generators (no larger than 2.0 MW each) or that with Figure 14 less than 1% of the buses have an ending voltage drop of more than 0.03 per unit. Also such plots provide no information on the associated buses' locations.

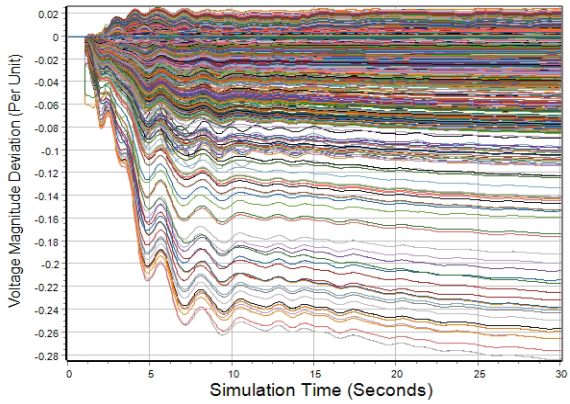

Figure 14: 82K Voltage Magnitude Response

There are a variety of different ways to present the results more geographically. While individual transmission lines and other objects (e.g., generators or substations) could be shown on a oneline, as indicated by Figure 3 the large number of objects makes this difficult, at least for an overview visualization. An alternative, shown in Figures 15 to 17, is to group the buses or substations and then visualize group values. In Figures 15 and 16 this is done using the approach of [18] in which the GDV objects (for substations here) are grouped geographically using a latitude and longitude grid, and then the object is drawn at the geographic average for the objects in the group. Also, for time-domain simulation results it is often helpful to show the deviation of the values compared to their original values rather than showing their absolute values.

For example in Figure 15, representing conditions at a simulation time of 2.0 seconds or 1.0 second after the contingency, the yellow and magenta rectangles show the change in the total real power generation within each grid location, with magenta used to show locations of decrease and yellow locations of increase. Each rectangle also shows a text value for the real power change, and the size of the rectangle is function of the generation change (with a linear scaling used except the rectangle sizes are capped for small and large values). Hence at a glance the location of the generator outage in Arizona is apparent. The approach of [19] can then be used to visualize the overall net change in the transmission line flows. Finally a bus voltage contour [32] is used to show the change in the bus voltage magnitudes. Figure 16 is identical to Figure 15 except it shows the results for a simulation time of 30.0 seconds. With these visualizations the location of the decreased voltages, shown graphically in Figure 14, are apparent.

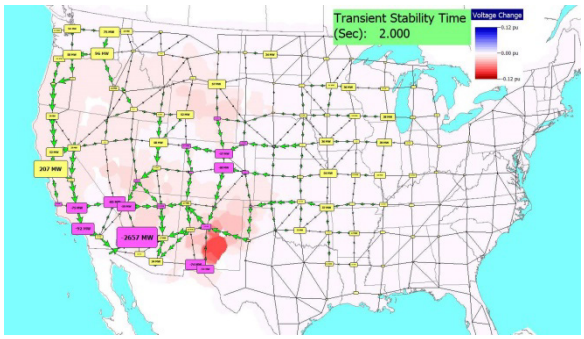

Figure 15: 82K Overall Response Visualization at 2.0 Seconds

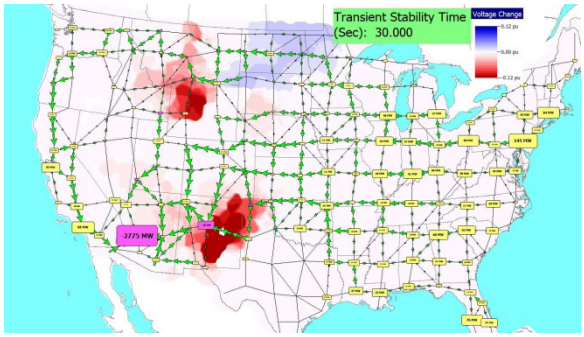

Figure 16: 82K Overall Response Visualization at 30.0 Seconds

Figure 17 shows results for the same scenario and is similar to the previous two figures except rather than grouping the substation values by their latitude and longitude they are grouped by their area. Then each area GDV is colored and sized to indicate the maximum change the voltage magnitude for all the buses in the area (all decreases here), labels are added to show the change in the aggregate line flows, and the contour shows the bus frequency.

5. Performance

The primary focus of this paper and its associated study is on understanding the stability considerations associated with a potential synchronous interconnection of large-scale electric grids. Given the

distinctiveness of the study, most of the engineering time had been focused on understanding and interpreting the results, as opposed to a focus on the performance of the simulation algorithm. Also, to give the best possible results, full detail dynamic models have been used for both the EI and WECC. Still, it is helpful to provide some performance results. For reference the results given here are based on simulations done using a PC with an Intel Core i7-5820K CPU running at 3.30 GhZ with 16 GB of memory using the Windows 10 Pro operating system.

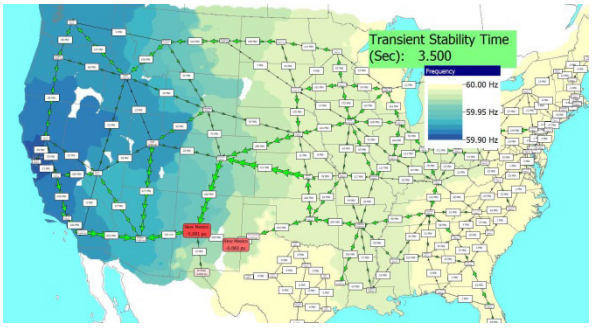

Figure 17: Alternative 82K Overall Response Visualization at 3.5 Seconds

Concerning execution speed, as noted in [33] for some commercial applications in which a wide variety of time-domain simulation contingencies need to be considered, since each contingency is independent of the others the application is naturally parallelizable with the execution speed dependent on the number of cores available, the number of contingencies and the speed to solve each contingency. Some such parallel studies were performed here, but at most only a few contingencies were run simultaneously. Each then ran on a single core. The execution time in seconds to perform a single second of simulation varied based on the size of the grid considered, the utilized models and the degree of variation in the system dynamics (with more quiescent times running the fastest and the times immediately after a contingency was applied the slowest). Ballpark ratios of execution time to simulation time are 20 for the 23K bus only WECC grid, 36 for the 82K bus synthetic grid, and 80 for the full 110K bus grid.

Concerning memory usage, the simulation environment used here provided great flexibility in terms of how many of the results are stored. Options included not storing any results (useful for running interactive simulations such as described in [34] but not used here except in the results given below), storing selected results fully in RAM, and storing selected results to a hard drive file. In addition, there is an option to store for selected time points the information sufficient to initialize a power flow solution or to visualize the results (called dynamic snapshots in [35]). Without storing any results the Windows reported memory usage was about 800 MB for the 23K grid, 2.2 GB for the 82K grid and 2.5 GB for the 110K grid. There is a progressive increase in memory usage only when results are stored in RAM or the dynamic snapshots are stored (also in RAM). A ballpark figure for the amount of memory used is about 70 bytes per bus per dynamic snapshot. The simulation environment allowed the rate at which the snapshots are saved to vary during the simulation. For example, once every 0.05 seconds for the first 10 seconds, then every 0.2 seconds for the next 20 seconds, then once per second for the remainder of the simulation. This approach was used in creating Figures 15 to 17, since the simulation could be run once, and then the particular time points displayed and visualized using the dynamic snapshots.

6. Conclusion

The paper has presented some of the stability considerations associated with a potential ac interconnection of the North American East and West electric grids. The paper's results are based on simulations done using a 110,000-bus model that joined the two grids with nine ties at locations where the two grids are already close. These ties had voltages ranging from 345 to 161 kV, and these interconnections could be done with quite modest changes to the existing transmission systems.

Based on doing many different time domain stability simulations, the conclusion is there are no technical showstoppers associated with doing such an interconnection, and that such an interconnection could be accomplished without the need to build a significant amount of new transmission. The limiting characteristic is that during generator loss contingencies in the WECC about 80% of the lost power will flow through the interface from the EI to the WECC. This is due to the governor response taking place uniformly through the grid, and that most of the generation (and the associated governor response) is on the EI side of the interface. This issue is fundamental to interconnecting large grids and does require any interface joining two such larger grids be able to handle this flow at least until the automatic generation control can respond. The paper also showed how newer visualization techniques can be used to help with interpretation of the simulation results.

Directions for future work include doing more simulations under a wider range of operating conditions and considering in more depth economic

and other non-technical issues associated with such an interconnection. There is also a need to consider how such a combined grid could be further strengthened through the addition of new, longer distance ac transmission and/or the construction of more HVDC.

6. Acknowledgements

This work was partially funded by the Southwest Power Pool through the PSERC project S-92G, by PSERC project S91, and by the US National Science Foundation through Award ECCS-1916142.

7. References

[1] J. Cohn, "When the grid was the grid: the history of North America's brief coast-to-coast interconnected machine [scanning our past]," *Proc. of the IEEE*, vol. 107, no. 1, pp. 232–243, 2019.

[2] N. Cohn, S. B. Biddle, R. G. Lex, E. H. Preston, C. W. Ross, and D. R. Whitten, "On-line computer applications in the electric power industry," *Proc. of the IEEE*, vol. 58, no. 1, pp. 78–87, 1970.

[3] A. L. Figueroa-Acevedo, "Opportunities and benefits for increasing transmission capacity between the US eastern and western interconnections," PhD Dissertation, Iowa State University, 2017.

[4] Y. Li and J. D. McCalley, "Design of a High Capacity Inter-Regional Transmission Overlay for the U.S." *IEEE Trans. on Power Systems*, vol. 30, pp. 513–521, 2015.

[5] M. A. Elizondo, N. Mohan, J. O'Brien, Q. Huang, D. Orser, W. Hess, H. Brown, W. Zhu, D. Chandrashekhara, Y. V. Makarov, D. Osborn, J. Feltes, H. Kirkham, D. Duebner, and Z. Huang, "HVDC macrogrid modeling for power-flow and transient stability studies in North American continental-level interconnections," *CSEE Journal of Power and Energy Systems*, vol. 3, no. 4, pp. 390–398, 2017.

[6] A. Bloom, J. Novacheck, G. Brinkman, J. McCalley, A.L Figueroa-Acevedo, A. Jahanbani-Ardakani, H. Nosair, A. Venkatraman, J. Caspary, D. Osborn, J. Lau, "The Value of Increased HVDC Capacity Between Eastern and Western U.S. Grids: The Interconnections Seam Study," NREL/JA-6A20-76580, NREL, October 2020.

[7] Western Area Power Administration, "East/West AC Intertie Feasibility Study," Tech. Report, 1994.

[8] *Western Area Power Adminstration's First 25 Yeas as a Power Marketing Agency*, WAPA, October 2002; available online at https://www.wapa.gov/newsroom/Publications/Documents/25yr-history_2.pdf

[9] J. Caspary, J. McCalley, S. Sanders, and M. Stoltz, "Proposed Eastern Interconnection and Western Electricity Coordinating Council Seams Study," in CIGRE US National Committee 2015 Grid of the Future Symposium, 2015, pp. 1–11.

[10] T.J. Overbye, K.S. Shetye, H. Li, W. Trinh, J. Wert, "Feasibility Assessment of Synchronous Operations of the North American Eastern and Western Interconnections," PSERC Publication 21-02, Jan. 2021.

[11] K.S. Shetye, T.J. Overbye, H. Li, J. Thekkemathiote, and H. Scribner, "Considerations for Interconnection of Large Power Grid Networks," IEEE Power and Energy Conference at Illinois, Champaign, IL, April 2021.

[12] "Critical Energy/Electric Infrastructure Information," US Federal Energy Regulatory Committee (FERC), June 2021; online at https://www.ferc.gov/ceii.

[13] A. B. Birchfield, T. Xu, K. M. Gegner, K. S. Shetye, and T. J. Overbye, "Grid structural characteristics as validation criteria for synthetic networks," *IEEE Trans. on Power Systems*, vol. 32, pp. 3258–3265, July 2017.

[14] T. Xu, A.B. Birchfield, K.S. Shetye, T.J. Overbye, "Creation of Synthetic Electric Grid Models for Transient Stability Studies," Proc. 10th Bulk Power Systems Dynamics and Control Symposium (IREP 2017), Espinho, Portugal, Sept. 2019.

[15] T. Xu, A.B. Birchfield, T.J. Overbye, "Modeling, Tuning and Validating System Dynamics in Synthetic Electric Grids," *IEEE Trans. on Power Systems*, vol. 33, pp. 6501-6509, Nov. 2018.

[16] *WECC Remedial Action Scheme Design Guide*, WECC, Dec. 2016; available at https://www.wecc.org/Reliability/RWG%20RAS%20Design%20Guide%20_%20Final.pdf

[17] T.J. Overbye, E.M. Rantanen, S. Judd, "Electric power control center visualizations using geographic data views," Bulk Power System Dynamics and Control -- VII. Revitalizing Operational Reliability -- 2007 IREP Symposium, Charleston, SC, August 2007, pp1-8.

[18] T.J. Overbye, J. Wert, K.S. Shetye, F. Safdarian, A.B. Birchfield, "The Use of Geographic Data Views to Help with Wide-Area Electric Grid Situational Awareness," Fifth Texas Power and Energy Conference, College Station, TX, February 2021.

[19] T.J. Overbye, J. Wert, K. Shetye, F. Safdarian, and A. Birchfield, "Delaunay Triangulation Based Wide-Area Visualization of Electric Transmission Grids," Kansas Power and Energy Conference (KPEC), Apr. 2021.

[20] electricgrids.engr.tamu.edu.

[21] IEEE PES Power System Dynamic Performance Committee, "Stability definitions and characterization of dynamic behavior in systems with high penetration of power electronic interfaced technologies, PES-TR77, April 2020.

[22] P. Kundur, J. Paserba, V. Ajjarapu, G. Andersson, A. Bose, C. Canizares, N. Hatziargyriou, D. Hill, A. Stankovic, C. Taylor, T. Van Cutsem, V. Vittal, "Definition and classification of power system stability ieee/cigre joint task force on stability terms and definitions," *IEEE Transactions on Power Systems*, Vol. 19, no. 3, pp. 1387–1401, Aug 2004.

[23] IEEE Subsynchronous Resonance Working Group, "Term, Definitions and Symbols for Subsynchronous Oscillations," *IEEE Trans. Power App. and Sys.*, Vol. PAS-104, pp. 1326-1334, June 1985.

[24] C. W. Gear, “Multirate Methods for Ordinary Differential Equations,” Department of Computer Science, University of Illinois at Urbana-Champaign, Report UIUCDCS-F-74-880, September 1974.
[25] C.W. Gear, D.R. Wells, “Multirate linear multistep methods”, *BIT,* vol. 24, pp. 484–502, 1984.
[26] M. Crow and J. G. Chen, “The multirate method for simulation of power system dynamics,” IEEE Transactions on Power Systems, vol. 9, no. 3, p. 1684–1690, August 1994.
[27] J.H. Yeo, W.C. Trinh, W. Jang, T.J. Overbye, “Assessment of Multirate Methods for Power System Dynamics Analysis,” 2020 North American Power Symposium, Tempe, AZ, April 2021.
[28] M. Luther, I. Biernacka, D. Preotescu et al., “Feasibility Aspects of a Synchronous Coupling of the IPS/UPS with the UCTE,” *CIGRE Session*, no. C1 204, 2010.
[29] W. Trinh, K.S. Shetye, I. Idehen, T.J. Overbye, "Iterative Matrix Pencil Method for Power System Modal Analysis," Proc. 52nd Hawaii International Conference on System Sciences, Wailea, HI, Jan. 2019.
[30] I. Idehen, B. Wang, K.S. Shetye, T.J. Overbye, J.D. Weber, "Visualization of Large-Scale Electric Grid Oscillation Modes," Proc. 2018 North American Power Symposium, Fargo, ND, Sept. 2018.
[31] T.J. Overbye, K.S. Shetye, J.L. Wert, W. Trinh, and A. Birchfield, “Techniques for Maintaining Situational Awareness During Large-Scale Electric Grid Simulations,” IEEE Power and Energy Conference at Illinois (PECI), Champaign, IL, April 2021.
[32] J.D. Weber and T.J. Overbye, "Voltage contours for power system visualization," *IEEE Trans. on Power Systems*, Vol. 15, pp. 404-409, February, 2000.
[33] National Academies of Sciences, Engineering, and Medicine, A*nalytic Research Foundations for the Next-Generation Electric Grid,* The National Academies Press, Washington, DC, 2016, doi:10.17226/21919.
[34] T.J. Overbye, Z. Mao, A.B. Birchfield, J.D. Weber, M. Davis, “An Interactive, Stand-Alone and Multi-User Power System Simulator for the PMU Time Frame,” Proc. 2019 Texas Power and Energy Conference, College Station, TX, February 2019.
[35] W. Trinh, Z. Mao, T. J. Overbye, J. D. Weber, and D. J. Morrow, “Considerations in the Initialization of Power Flow Solutions from Dynamic Simulation Snapshots”, 2020 North American Power Symposium (NAPS 2020), Tempe AZ, April 2021.